Dependence of InGaN/GaN LED emission spectrum parameters on the value of injection current

© A.V. Igo, L.N. Vostretsova, V.A. Ribenek

Ulyanovsk State University,
432063 Ulyanovsk, Russia

E-mail: igoalexander@mail.ru

Received December 23, 2024
Revised March 9, 2025
Accepted April 17, 2025

The emission spectra of InGaN/GaN LEDs with quantum wells for injection currents from 1 μA to 55 mA have been measured. The dependence of the parameters of the radiation spectrum on the magnitude of the current is analyzed using a model when the process of electron injection into the quantum well region was considered as a nonequilibrium stationary process. Modeling has determined that a decrease in the quantum yield at high currents is associated with a decrease in the lifetime of current carriers due to an increase in temperature in the region of the $p-n$ junction due to Joule heat. The temperature in the region of the $p-n$ junction was estimated from the width of the radiation spectrum, by modeling the volt-ampere characteristics, from the high-energy slope of the radiation spectrum, and by measuring the luminescence spectra of Cr^{3+} ions on a sapphire substrate. At an ambient temperature of 23 °C with a current of 55 mA, the temperature in the region of the quantum well is estimated to be 97 °C, in the region of the $p-n$ junction 60 °C, and the sapphire substrate 45 °C. Modeling has shown that by measuring the dependence of the shift of the maximum of the radiation spectrum on the magnitude of the current, it is possible to determine the most important parameters of the InGaN/GaN structure with quantum wells.

Keywords: InGaN/GaN, quantum well structures, radiation efficiency, spectrum modeling.

DOI: 10.61011/SC.2025.01.61072.7485

1. Introduction

Due to technological progress in the field of epitaxial growth of GaN-based heterostructures, InGaN/GaN-based light-emitting diodes and lasers have been widely used as light sources [1]. Quantum yield that characterizes conversion of electric energy into light is the essential parameter of light-emitting devices. Studies show that the quantum yield of InGaN/GaN LEDs decreases as the current density increases. The basics of statistics and recombination of injected carriers in InGaN/GaN LEDs with active quantum-size region were established within the drift-diffusion and ABC models and described in numerous works, e.g. in [2].

Experimental and theoretical studies show that decrease in the quantum yield with growing current density is caused by heating of the $p-n$ junction, injection drop, charge carrier delocalization and Auger recombination [3–7].

Simulation of radiating capacity and radiation spectrum is an important research method. Simulation is carried out to compare theoretical models with parameters of the spectrum observed in the experiment such as intensity, spectral line width, energy of the peak of spectral line. In particular, the purpose of simulation is to compare the parameters of theoretical models with clear physical meaning and of experimentally measured radiation spectra. Good agreement with the experiment was obtained when using a theoretical model containing 4 and more parameters [8–10].

Investigation of the dependence of radiation intensity and other radiation spectrum parameters on the magnitude of injection current is an important experiment, one of the goals of which is to determine the dependence of radiating capacity and compare it with the parameters of theoretical models.

Consideration of numerous factors affecting the decrease in quantum yield with growing current density leads to complication of the model and need to introduce additional parameters. In particular, using the density of states function model, that takes in account fluctuations of crystal-field potential in [8,9], improves considerably the agreement between the model and experiment.

The objective of this work is to study the effect of injection level on the InGaN/GaN LED radiation spectra and to compare the radiation spectra parameters with the theoretical model.

2. Test samples and measurement data

The experiment measured radiation spectra of packageless blue LEDs (Taiwan Oasis Technology Co., Ltd) with 5 quantum wells (QW) based on InGaN solid solution. GaN layers were grown on a sapphire substrate (0001) using a metalorganic chemical vapor deposition (MOCVD) system. The InGaN/GaN LED structure consists of a GaN buffer layer grown at low temperature, GaN n-type layer, active InGaN/GaN quantum well region and GaN p-type layer. Indium tin oxide (ITO) is applied to the GaN p-type layer to form a transparent conducting layer.

Spectra were measured using the MSD-2 advanced monochromator and FEU-100 photomultiplier tube. In

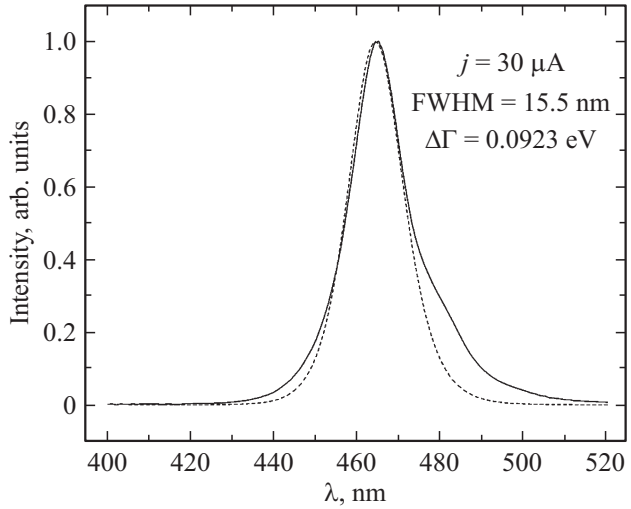

Figure 1. LED radiation spectrum at 30 μA, $T = 23\,^{\circ}$C (solid line). Curve of function (8) for 23 °C (dashed line). Spectral line width is 0.0923 eV.

the experiment, spectral slit width of the monochromator was 0.1 nm. To measure temperature dependences of the spectrum parameters, the LED was placed into a thermostat at a temperature kept within 0.1 °C using the TRM-01 temperature controller. Radiation from the LED to monochromator was collected using a flexible optical waveguide.

Experimental measurements were performed with constant current set in the range from 1 μA to 55 mA, which corresponded to current densities from $2.5 \cdot 10^{-4}$ A/cm^2 to 13.8 A/cm^2. LED crystal area is 0.4 mm^2. A total of 5 LEDs from the same batch were examined. All measurement data coincided. As an example, Figure 1 shows a LED radiation spectrum at 30 μA. The recorded spectra were analyzed using Origin 8 to determine the spectral line parameters. For each spectrum, position of the peak $\varepsilon_{\max}$ and FWHM of the spectral line $\Delta\Gamma$ were determined. The spectral line intensity was determined as the area under the spectral profile.

Dependences of particular spectrum parameters on the magnitude of injection current are shown in Figures 2 and 3. Measurements show that as the current flowing through the LED increases, increase in the radiation intensity, shift of the peak of radiation spectrum towards shorter wavelengths (higher energies) and increase in the spectral line width are observed.

3. Simulation of the LED radiation spectrum parameters

3.1. Shift of the peak of radiation spectrum

Radiation intensity is generally associated with the concentration of injected electrons by relations described by the ABC model [5]. Let's consider a simplified simulated situation when electrons are injected into the region where holes are the majority charge carriers (p-region), radiation intensity I in this case is limited by the number of injected electrons n':

$$I = \alpha n'. \tag{1}$$

Here, α is the coefficient. The number of carriers in the band may be represented using the electron distribution function in the zone by energies $f(\varepsilon)$ and density of states function $g(\varepsilon)$:

$$n = \int f(\varepsilon) g(\varepsilon) d\varepsilon. \tag{2}$$

Electron injection and motion in the conduction band exposed to an electric field may be addressed as a non-equilibrium stationary process. For such approach, electron

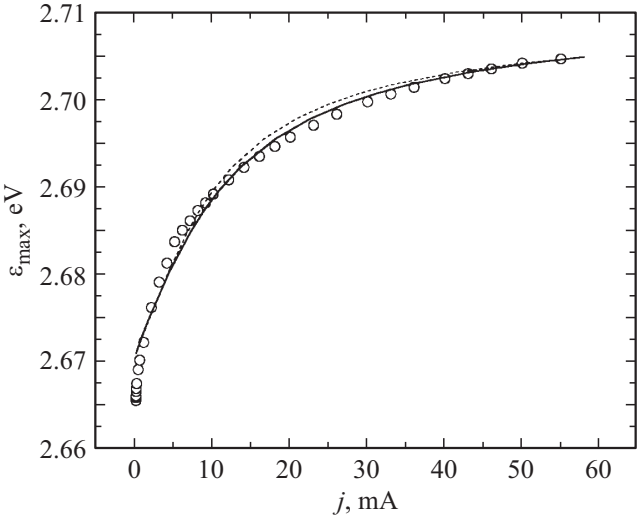

Figure 2. Energy of the peak of radiation spectrum vs. current: dots — experiment, solid and dashed lines — calculation using equation (6).

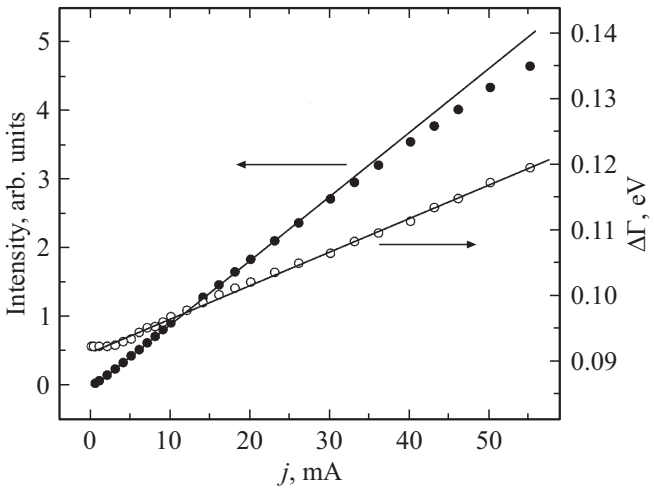

Figure 3. Radiation spectrum parameters vs. current: intensity (solid circles), spectral line width (empty circles). Straight lines are shown for clarity.

distribution function in the band may be written as a sum of equilibrium function and non-equilibrium additive [11]:

$$f(\varepsilon) = f_0(\varepsilon) + f_1(\varepsilon) = f_0(\varepsilon) + \frac{\partial f_0}{\partial \varepsilon}\Delta\varepsilon, \qquad (3)$$

$$f_0(\varepsilon) = \frac{1}{1+\exp\left(\frac{\varepsilon-\varepsilon_F}{kT}\right)}.$$

$f_0(\varepsilon)$ is the equilibrium Fermi–Dirac function and ε_F is the equilibrium Fermi energy, $f_1(\varepsilon)$ is the non-equilibrium additive that is proportional in linear approximation to $\Delta\varepsilon$ — additional electron energy in the band that is received by the electron moving under the action of an external field applied to the diode.

Number of electrons injected into the conduction band n' and injection current will be defined by the non-equilibrium additive of the distribution function:

$$n' = \int f_1(\varepsilon) g(\varepsilon) d\varepsilon, \;\; j = e\int v(\varepsilon) f_1(\varepsilon) g(\varepsilon) d\varepsilon. \qquad (4)$$

Electron dispersion law in conduction band $\varepsilon(v)$ for a particular semiconductor is known, it may be used to determine the rate and density of states in the band: $v(\varepsilon), g(\varepsilon)$. Calculation of integrals (4) taking into account (3) results in a simple linear dependence of the number of carriers and current on $\Delta\varepsilon$

$$j = \beta\Delta\varepsilon, \quad n' = \gamma\Delta\varepsilon. \qquad (5)$$

Relation (1) taking into account (5) is expressed in that the simulated radiation intensity depends linearly on the magnitude of injection current. In the experiment, the radiation intensity is close to a linear dependence in a sufficiently wide current range (Figure 3).

Diode radiation spectrum $w(\varepsilon)$ depends on the distribution of electrons and holes by energies and density of states in bands. Taking into account the fact that electrons are injected into the band where holes are the majority charge carriers (p-region), and the electrons themselves are minority carriers in this band, then the radiation intensity is limited by the number of injected electrons, and the radiation spectrum will depend on energy distribution of electrons only, i. e. on subintegral function of equation (2), and the peak of spectrum ε_{max} may be found from

$$w(\varepsilon) = f(\varepsilon) g(\varepsilon), \quad \frac{\partial w(\varepsilon)}{\partial \varepsilon} = 0. \qquad (6)$$

Coordinate confinement of an electron (quantum well) leads to a known modification of the spectrum and density of allowed electron states in the conduction band. In case of an ideal quantum well, the density of states may be written as a sum:

$$g(\varepsilon) = G\sum_i Q(\varepsilon - \varepsilon_i).$$

$Q(x)$ is the Heaviside function, ε_i are the quantum well energy levels. For low injection levels, one level ε_1 is sufficient and the density of states is described by the step:

$$g(\varepsilon) = \begin{cases} G, & \varepsilon > \varepsilon_1, \\ 0, & \varepsilon < \varepsilon_1. \end{cases}$$

In real systems, nonuniformity of material composition and layer thickness causes a spread of values of ε_1 within the material. Assuming a normal distribution of the spread around ε_1 with dispersion ε_0, then the resulting density of states will be described by a convolution of the Heaviside function with the normal distribution function and may be expressed through an error function:

$$g(\varepsilon) = G\int_{-\infty}^{+\infty} Q(\varepsilon-\varepsilon_1)\frac{1}{\sqrt{2}\varepsilon_0}\exp\left[-\left(\frac{x-\varepsilon_1}{\sqrt{2}\varepsilon_0}\right)^2\right]dx$$

$$= G\,Erfc\left(\frac{\varepsilon-\varepsilon_1}{\sqrt{2}\varepsilon_0}\right). \qquad (7)$$

In the quantum well, ε_1 is the lower-energy allowed electron state. With the minimum experimental injection level of $1\,\mu$A, additional electron energy in the band (quantum well) will be assumed equal to zero ($\Delta\varepsilon = 0$). While the experimental peak of radiation spectrum intensity corresponds to $\varepsilon_{max} = 2.665$ eV (Figure 2). Then for this case, by solving (6) for the equilibrium distribution function at set values of ε_1 and ε_0, the magnitude of equilibrium Fermi energy ε_F may be defined. This value is further used for calculation of non-equilibrium distribution function (3). Then, by setting various values of $\Delta\varepsilon$ and solving equations (6), we get the design dependence $\varepsilon_{max}(\Delta\varepsilon)$.

Dashed lines in Figure 2 show the calculation of $\varepsilon_{max}(\Delta\varepsilon)$ at room temperature with $\varepsilon_1 = 2.66$ eV, $\varepsilon_F = 2.702$ eV and $\varepsilon_0 = 0.08$ eV. For comparison with the experiment, linear correlation between $\Delta\varepsilon$ and current using equation (5), β was chosen by fitting and is equal to 0.318 A/eV. The curve shows good coincidence between the design dependence and experiment.

Determination of ε_1 and ε_0 for the model of density of states function (7) by fitting to the experimental dependence is of practical importance. In particular, experimental determination of these parameters will provide an independent method for comparison of nanoscale layer geometries when making a quantum well (from ε_1) and manufacturing tolerance of material composition and layer thickness (by ε_0). Some works [8–10,12] used the following function as a density of states function

$$g(\varepsilon) = \frac{G}{1+\exp\left(\frac{\varepsilon-\varepsilon_1}{\varepsilon_2}\right)}.$$

This function can be also used to describe $\varepsilon_{max}(\Delta\varepsilon)$. When $\varepsilon_2 = 0.65\varepsilon_0$ is chosen, calculation data fully coincides.

3.2. Spectral line width

The experimental width of spectral line increases as the current grows almost across the entire the current range, except the range of < 1 mA. In the non-equilibrium distribution function model, non-equilibrium electron gas temperature in the conduction band is a parameter defining

the width of radiation spectral line. The non-equilibrium additive $f_1(\varepsilon)$ is a bell-shaped function that is very close to the shape of LED radiation spectrum with a peak at ε_F and a temperature-dependent width:

$$f_1(\varepsilon) = \frac{\partial f_0}{\partial \varepsilon}\Delta\varepsilon = \frac{\Delta\varepsilon}{kT}\frac{\exp\left(\frac{\varepsilon-\varepsilon_F}{kT}\right)}{\left(1+\exp\left(\frac{\varepsilon-\varepsilon_F}{kT}\right)\right)^2}. \quad (8)$$

For room temperature ($kT = 0.026$ eV) and $\varepsilon_F = 2.7$ eV, FWHM of the function is 0.0923 eV, which coincides with the spectral line width of the LED at low injection current. In Figure 1, the normalized $f_1(\varepsilon)$ is converted into $f_1(\lambda)$ and shown as a dashed line for comparison with the measured radiation spectrum at 30 μA.

Increase in the injection current leads to the growth of the spectral line width (Figure 3). This increase in the width may be associated with the electron gas temperature growth in the conduction band. For 55 mA (high injection level), the width is 0.1194 eV. According to equation (8), such width corresponds to the electron gas temperature of $kT = 0.032$ eV, i.e. the temperature increased to 100 °C.

For low current (30 μA), when gas may be considered as equilibrium and its temperature closely corresponds to the ambient temperature, radiation spectra were measured in the temperature range from 23 °C to 100 °C. The measurements showed that $\Delta\Gamma$ and peak of the radiation spectrum in this temperature region might be approximated by linear temperature dependences:

$$\Delta\Gamma = 0.0796 + 0.412\cdot 10^{-4}T\ ^\circ\mathrm{C},$$

$$\varepsilon_{\max} = 2.674 - 2.67\cdot 10^{-4}T\ ^\circ\mathrm{C}. \quad (9)$$

According to dependence (9), spectral line width for 55 mA equal to 0.1194 eV corresponds to the diode temperature of 97 °C. Estimated temperature according to (8) agrees well with measurement data (9). Such experiment supports the assumption that the electron gas temperature in the conduction band increases with the injection current. Comparing measurements (9) and the dependence of the spectral line width on current (Figure 3), we get the correlation between current and electron gas temperature in the conduction band:

$$kT = 0.026 + 1.1\cdot 10^{-4}j. \quad (10)$$

3.3. Radiation intensity

The observed deviation from the linear dependence for radiation intensity (Figure 3) may be also associated with the increase in the electron gas temperature in the conduction band. LED radiation efficiency may be characterized by the ratio of intensity to current. Recalculated I/j from Figure 2 is shown in Figure 4. The curve has its peak followed by a dip as the injection current increases. It follows from equations (1) and (5) that

$$I = \alpha\gamma\Delta\varepsilon. \quad (11)$$

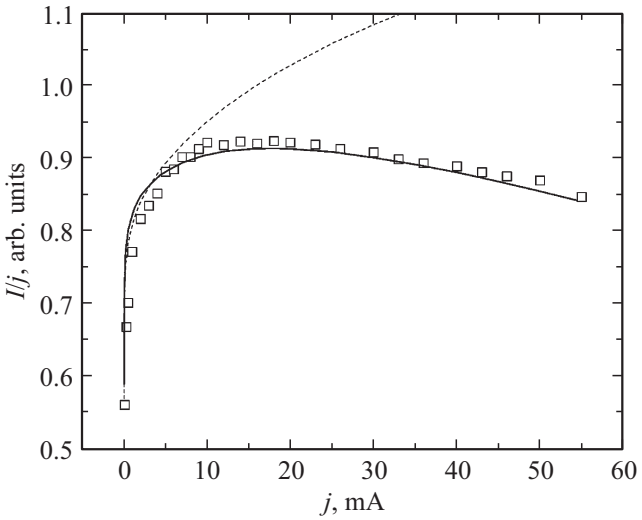

Figure 4. Dependence of LED radiation efficiency I/j on current: dots — experiment, dashed line — calculation as per (11), solid line — calculation as per (11) taking into account (13).

Utilization of a simple linear correlation between $\Delta\varepsilon$ and j with constant β (5) leads to the fact that I/j is independent of current, which contradicts the experiment. Additional electron energy $\Delta\varepsilon$ received in motion when the electron is exposed to the external field is proportional to the electric energy power and electron lifetime τ, during which the electron can receive this power:

$$\Delta\varepsilon = \delta U j\tau, \quad (12)$$

U is the voltage, δ is the coefficient of proportionality. Comparing (12) with (5), we obtain that β depends on the LED voltage and carrier lifetime in the band. Dependence of voltage on current for the LED $U(j)$ is shown in Figure 5. Calculation of I/j as per (11) and (12) taking into account the experimental data for $U(j)$ is shown in Figure 4 as a dashed line. The difference between the calculated and experimental dependences in the high injection level region may be caused by the decrease in the current carrier lifetime τ as the temperature at the $p-n$ junction increases. Investigations of the temperature effect on the carrier scattering in the InGaN quantum well show that, for temperatures about 300 K and higher, the temperature dependence of scattering on optical phonons produces the highest effect [13]. Temperature effect on other scattering mechanisms in this temperature region appears to be much lower [13,14]. The temperature dependence of electron lifetime in this case may be written as

$$\tau = \tau_0(kT)^{-m}. \quad (13)$$

For bulk semiconductors, the power exponent for polar optical phonons $m = 1.5$ [11], the experiment in quantum wells for 2D electron gas shows $m = 2$ [14]. Calculation of (11) taking into account $U(j)$, (13) and (10) is shown in Figure 4 as a solid line. The calculation data agrees

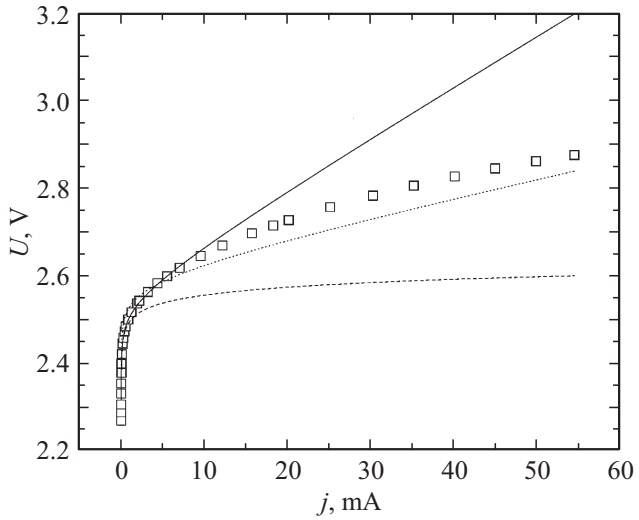

Figure 5. LED's current-voltage curve: dots — experiment, dashed line — calculation of the ideal $p-n$ junction model at a constant temperature of 23 °C, solid line — taking into account LED heating due to current flow according to model (10), dashed line — taking into account LED heating according to the sapphire substrate temperature measurement data.

most effectively with the experimental results for $m = 1.7$. Simulation data agrees well with the assumption that the electron gas temperature increases in the LED conduction band under action of the flowing current.

Basically, $U(j)$ in Figure 5 also indicates that the temperature at the $p-n$ junction region increases as the current grows. Figure 5 shows CVC approximations by the ideal $p-n$ junction model:

$$j = j_0\left(\exp\left(\frac{U-U_0}{kT}\right)-1\right) \qquad (14)$$

for a constant temperature of 23 °C (dashed line) and with variable temperature depending on the current as per (10) (solid line). To fit (14) to the experiment, $U_0 = 1.7$ V and $j_0 = 2\cdot 10^{-13}$ mA were used.

Simulated temperature dependence (10) derived from the measured spectral line width differs from the temperature dependence that may be obtained from the ideal $p-n$ junction model (14). For 55 mA, the electron gas temperature in the radiative recombination region as per (10) is equal to 97 °C. For the measured $U = 2.88$ V for 55 mA as per model (14), the temperature at the $p-n$ junction is 60 °C. In the current range up to ~ 10 mA, both models agree well together: thus, for 10 mA, both models provide a temperature that is higher than room temperature by 13 °C. Difference in the calculated temperatures for high currents may be explained by the increase in current crowding within the $p-n$ junction area [15,16]. Investigations of the $p-n$ junction area in LEDs using the IR thermal-imaging microscopy method show that, when current densities are significant, uneven current density leads to temperature gradients that reach several tens of degrees even in optimized designs.

We use the method for determining the temperature at the $p-n$ junction by the slope of the short-wavelength (high-energy) side of the LED radiation spectrum [17]. This method is based on the assumption that the non-equilibrium carrier distribution function in the active layer has an exponential decay in the high energy region. In this case, reciprocal derivative of this function shall depend only on the electron gas temperature. This value is actually affected by numerous factors, nevertheless this method is used in many cases and provides a correct result. To calculate the temperature, reciprocal derivative of the intensity logarithm of photon energy is calculated:

$$T_{id}(\Delta) = \left(k_{\mathrm{B}}\frac{\partial \ln I}{\partial h\nu}\Big|_{\Delta}\right)^{-1}.$$

Derivative is calculated at point Δ located at a distance from the peak of spectrum intensity $\Delta = h\nu - \varepsilon_{\max}$. The obtained value may be used to calculate the temperature in Kelvin degrees using the calibration factors:

$$T(\mathrm{K}) = T_0 + mT_{id}.$$

Calibration factors T_0 and m are determined by measuring spectra at a known temperature. Figure 6 shows the calculation of $T_{id}(\Delta)$ for spectra measured at the injection currents of 30 μA, 30 mA, 40 mA and 55 mA. To calculate the calibration factors, Figure 6 shows the calculation of $T_{id}(\Delta)$ for 30 μA at two temperatures: 23 °C and 83 °C. Solid lines are drawn through the points for clarity (second-order polynomial, fitting by the least-square method).

T_{id} calculated by the spectra measured at low current (calibration spectra) at Δ from 0.03 eV to 0.09 eV is constant and, therefore, the injected electron distribution function actually has an exponential decay in this energy

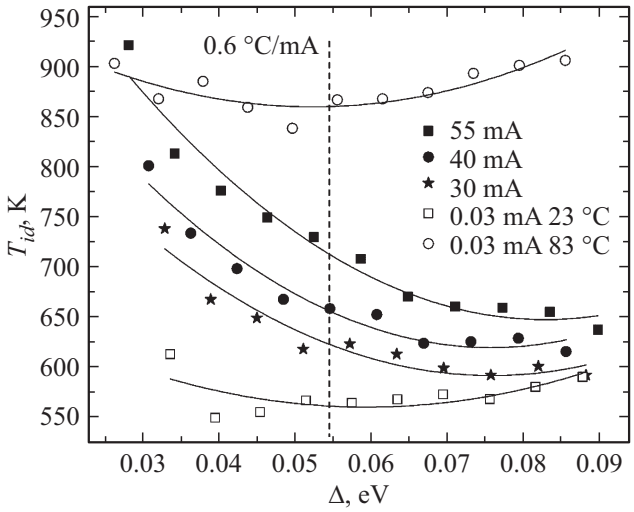

Figure 6. Temperature determined by the slope of the short-wavelength side of the LED radiation spectrum. See the text for explanations.

area. Using this data, we get $m = 0.16$, $T_0 = 216$ K. At high injection currents (30 mA and higher), T_{id} demonstrates the dependence on Δ in this energy region, therefore, the electron distribution function in the energy region has non-exponential decay and cannot be correctly characterized by one temperature value. This implies that there is a temperature gradient in the radiative recombination region. By the variation of T_{id} for 55 mA, 40 mA and 30 mA, it can be determined that the temperature variation with the increase in current is equal to 0.6 °C/mA almost across the entire range of Δ, which may be due to the fact that the temperature gradient formed at 30 mA doesn't vary considerably as the temperature increases. From the minimum current and to 30 mA, the temperature gradient grows. Using m and T_0, we obtain that at 55 mA the temperature in the radiative recombination region may be estimated from 91 to 47 °C.

Temperature may be calculated by the independent method of InGaN/GaN structure for different currents using the measured luminescence spectra of Cr^{3+} ions of the sapphire substrate. In [18], it was determined that the temperature increases linearly with the coefficient from 0.95 to 1.2 K/mA in the current range of 0–100 mA depending on the type of LED and measurement conditions.

To determine the temperature at the p–n junction, photoluminescence (PL) spectra of Cr^{3+} ions of the sapphire substrate were measured. PL spectra were measured using the DFS-52 advanced spectrometer in the range from 14 360 to 14 460 cm^{-1} at 1 cm^{-1} steps, the spectral slit width was 3 cm^{-1}. For PL excitation, a 532 nm 20 mW laser was used. Spectra were measured by applying the current from 0 mA to 55 mA at 10 mA steps to the LED. Peaks of the spectral lines R_1 and R_2 shifted to the low frequency region when the current increased from 0 mA to 55 mA. PL spectra for 0 mA and 55 mA are shows in Figure 7.

For each current, the frequency of the peak of spectral lines was determined as the frequency of the peak of a Lorentz profile that approximated the experimental spectral line in the best possible way. Using the approximation of the frequency of R_1 and R_2 from the temperature [19], we obtain that the sapphire substrate temperature increases linearly as the flowing current increases with the coefficient of 0.4 °C/mA. In particular, in Figure 7, the shift of frequencies of R_1 and R_2 is 3 cm^{-1} as the current increases by 55 mA, which corresponds to heating by 22 °C.

A dashed line in Figure 5 shows the calculated current-voltage curve when using the sapphire substrate temperature measurement data. Using the temperature dependence with 0.4 °C/mA is much closer to the experimental data and the obtained temperature of 45 °C is close to the estimated temperature as per model (14), taking into account that 60 °C was estimated exactly for the p–n junction region of the InGaN/GaN structure that is located at a distance, regardless of the fact that it is in a thermal contact with the sapphire substrate.

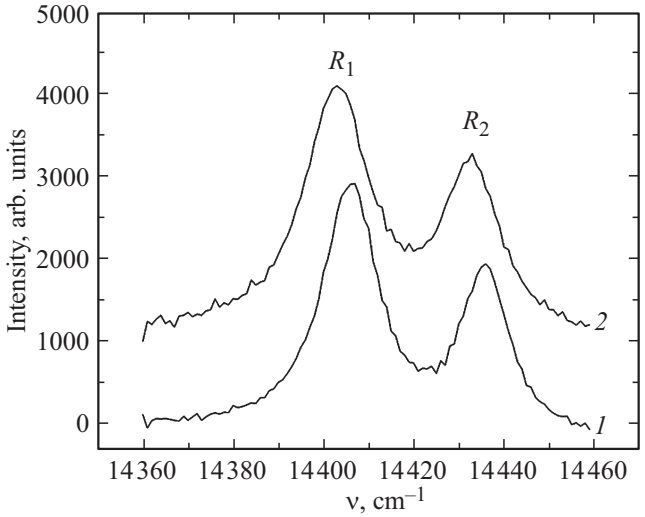

Figure 7. Photoluminescence spectra of Cr^{3+} ions of the sapphire substrate for two currents, mA: *1* — 0, *2* — 55. Shift of R_1 and R_2 is 3 cm^{-1}.

3.4. Temperature correction of the intensity peak dependence

Analysis of the temperature dependence makes it possible to correct the comparison between the calculated and experimental $\varepsilon_{\max}(\Delta\varepsilon)$ taking into account that β in (5) implicitly depends on the current:

$$\beta = 1/\delta U\tau.$$

Dependence of β on the current is inverse to I/j shown in Figure 4. Taking into account that the current in the experiment varies by almost 5 orders, the estimate of β as a constant value (varies in the order of 10%) is valid and, as shown in Figure 2, calculation of $\varepsilon_{\max}(j)$ agrees well with the experiment. To correct the calculation, it is necessary to consider the dependence of the InGaN band gap (energy level ε_1 of the quantum well) on the temperature (12) and the temperature itself in (3). Dependences (6) and (10) were used for a new calculation of $\varepsilon_{\max}(\Delta\varepsilon)$ and comparison with the calculated current $j = \beta\Delta\varepsilon$, where β was determined by the experimental data (dots in Figure 4). The resulting $\varepsilon_{\max}(j)$ is shown in Figure 2 as a solid line. Calculation parameters: $\varepsilon_1 = 2.641$ eV, $\varepsilon_F = 2.706$ eV, $\varepsilon_0 = 0.08$ eV.

4. Conclusion

For analysis of the radiation spectra parameters, the study used an approach that treated the electron injection into the quantum well region as a non-equilibrium stationary process. The non-equilibrium electron distribution function was written as a sum of the equilibrium function and non-equilibrium additive. The non-equilibrium additive is proportional to an additional energy received by the

conduction band electrons during movement when exposed to the external electric field.

As the current through the LED increases, the radiation intensity increased in a nearly linear fashion. The maximum nonlinearity of the dependence is in the low current region and is associated with the features of the LED's current-voltage curve in the low current region. Nonlinearity of the dependence and decrease in the radiation efficiency at high currents are associated with the decrease in the carrier lifetime as the temperature at the $p-n$ junction increases due to the Joule heat. Temperatures at the quantum well and $p-n$ junction were estimated by the radiation spectrum width using current-voltage curve simulation, by the slope of the short-wavelength side of radiation spectrum and by measuring the luminescence spectra of Cr^{3+} ions of the sapphire substrate. At the ambient temperature of 23 °C and injection current of 55 mA, the estimated temperature was 97 °C at the quantum well, 60 °C at the $p-n$ junction, and 45 °C for the sapphire substrate.

As the injection current increased, the peak of the radiation spectrum shifted to the higher light quantum energy region. Simulation showed that the shift of the peak of the radiation spectrum was induced by the restricted density of states in the band. A model is provided to correlate the shift of the peak with the parameters characterizing the quantum well ($\varepsilon_1, \varepsilon_0$) and doping level ($\varepsilon_F$). An equation of the density of states in the quantum well is proposed taking into account the mean low energy level in the quantum well and the degree of dispersion. A condition was determined, under which the proposed equation was equivalent to a widely used empirical equation.

Conflict of interest

The authors declare that they have no conflict of interest.

References

[1] E.F. Schubert. *Light Emitting Diodes* (Cambridge University Press, 2006).
[2] K.A. Bulashevich, V.F. Mymrin, S.Yu. Karpov, I.A. Zhmakin, A.I. Zhmakin. J. Comput. Phys., **213**, 214 (2006).
[3] A.A. Efremov, N.I. Bochkareva, R.I. Gorbunov, D.A. Lavrinovich, Yu.T. Rebane, D.V. Tarkhin, Yu.G. Schroeter. FTP, **40**, 621 (2006). (in Russian).
[4] J. Cho, E.F. Schubert, J. Kim. Laser Photon. Rev., **7**, 408 (2013).
[5] S. Karpov Optical Quant. Electron., **47**, 1293 (2015).
[6] J. Piprek. Appl. Phys. Lett., **107**, 031101 (2015).
[7] K. Bulashevich, S. Karpov. Phys. Status Solidi C, **5**, 2066 (2008).
[8] M.L. Badgutdinov, A.E. Yunovich, FTP, **42** (438) (2008).
[9] K.G. Zolina, V.E. Kudryashov, A.N. Turkin, A.E. Yunovich. FTP, **31**, 1055 (1997). (in Russian).
[10] V.E. Kudryashov, S.S. Mamakin, A.N. Turkin, A.E. Yunovich, A.N. Kovalev, F.I. Manyakhin. FTP, **35** 861 (2001). (in Russian).
[11] A.I. Ansel'm. *Vvedenie v teoriyu poluprovodnikov* (M., 1978). (in Russian).
[12] R. Chingolani, W. Stolz, K. Ploog. Phys. Rev. B, **40**, 2950 (1989).
[13] F. Sonmeza, E. Arslanb, S. Ardalid, E. Tirasa, E. Ozbay. J. Alloys Compd., **864**, 158895 (2021).
[14] K. Lee, M.S. Shur. J. Appl. Phys., **54** (11), 6432 (1983).
[15] A.E. Chernyakov, K.A. Bulashevich, S.Y. Karpov, A.L. Zakgeim. Phys. Status Solidi A, **210**, 466 (2013).
[16] A.L. Zakheim, G.L. Kuryshev, M.N. Mizerov, V.G. Polovinkin, I.V. Rozhansky, A.E. Chernyakov. FTP, **44**, 390 (2010). (in Russian).
[17] Z. Vaitonis, P. Vitta, A. Zukauskas. J. Appl. Phys., **103**, 093110 (2008).
[18] C. Winnewisser, J. Schneider, M. Borsch, H.W. Rotter. J. Appl. Phys., **89**, 3091 (2001).
[19] D.D. Ragan, R. Gustavsen, D. Schiferl. J. Appl. Phys., **72**, 5539 (1992).

Translated by E.Ilinskaya